REPORT DOCUMENTATION PAGE

AFRL-SR-BL-TR-99-

0069

1. AGENCY USE ONLY *(Leave blank)*	2. REPORT DATE	3. REPORT TYPE AND DATES COVERED
		01 Jul 97 - 31 Jul 98 Final

4. TITLE AND SUBTITLE
SBIR-97 (BMDO) OPTICAL RANDOM ACCESS MEMORY

5. FUNDING NUMBERS
62173C
1660/01

6. AUTHOR(S)
Dr Johnson

7. PERFORMING ORGANIZATION NAME(S) AND ADDRESS(ES)
Templex Technology
400 East 2nd Avenue Suite 101
Eugene OR 97401

8. PERFORMING ORGANIZATION REPORT NUMBER

9. SPONSORING/MONITORING AGENCY NAME(S) AND ADDRESS(ES)
AFOSR/NE
801 North Randolph Street Rm 732
Arlington, VA 22203-1977

10. SPONSORING/MONITORING AGENCY REPORT NUMBER
F49620-97-C-0036

11. SUPPLEMENTARY NOTES

12a. DISTRIBUTION AVAILABILITY STATEMENT
APPROVAL FOR PUBLIC RELEASED; DISTRIBUTION UNLIMITED

12b. DISTRIBUTION CODE

13. ABSTRACT *(Maximum 200 words)*

Our analyses of potential performance and cost structure during Phase I have been very positive. Based on these analyses, we believe that we can build a device that has an enormous performance advantage relative to magnetic storage media with a cost per GByte that is significantly below the cost per GByte of semiconductor DRAM. We were very encouraged by these results and have rapidly moved beyond the paper-based analyses to design and construction of an initial laboratory-demonstration unit, which we had orignially planned to begin during Phase II.

14. SUBJECT TERMS			15. NUMBER OF PAGES
			16. PRICE CODE
17. SECURITY CLASSIFICATION OF REPORT	18. SECURITY CLASSIFICATION OF THIS PAGE	19. SECURITY CLASSIFICATION OF ABSTRACT	20. LIMITATION OF ABSTRACT
UNCLASSIFIED	UNCLASSIFIED	UNCLASSIFIED	UL

Final Report for SBIR Contract F49620-97-C-0036

entitled

Optical Random Access Memory

Alan E. Johnson, Eric S. Maniloff, Thomas W. Mossberg

Templex Technology Corporation
400 E. 2nd Ave., Suite 101
Eugene, OR 97401

Templex Technology Corporation
Final Report of September 16, 1998
Period covered: July 1, 1997 – July 31, 1998
Project Title: " Optical Random Access Memory"

Background and Introduction

Data storage is a key component of any nontrivial computing system. Achievable computational performance strongly reflects limitations inherent in the storage technologies currently available. Crucial performance characteristics of data storage devices include

- random access latency time
- peak data transfer rate
- total capacity
- persistence time
- cost per unit performance.

In current desktop, server and high performance computing applications, overall data storage functionality is achieved through a combination of technologies, wherein the strengths of one technology compensate for the weaknesses of others. This situation has arisen because no single storage technology can provide optimal performance in all arenas. Two memory technologies currently dominate high performance storage applications: semiconductor RAM and mechanically accessed magnetic devices. Other technologies are important for archival backup (tape) and distribution (CD-ROM). Semiconductor RAM is very fast in terms of transfer rate (multi-Gigabit/second bus aggregate) and random access time (50-100 nanoseconds). However, it is expensive and usually volatile. Mechanically accessed magnetic storage devices offer enormous (over 10 Gigabytes/unit) permanent storage for a very low price, but have very long (5-10 millisecond) random access latency times and relatively low peak transfer rates (100-200 Megabit/second serial).

The mismatch in performance (speed and capacity) between magnetic storage devices and semiconductor RAM leads to performance bottlenecks in many computational applications, especially those applications that require access to large numbers of small data records. It is exactly this bottleneck that Templex Technology is addressing through the development of a new memory technology, Optical Dynamic RAM (ODRAM). In a simple implementation, ODRAM is a two dimensional memory with data stored in an array of spatial locations. At first glance, this seems conceptually similar to standard magnetic or optical disk technology. However, in ODRAM, *many thousands of bits are stored in each and every spatial location*, through the techniques of persistent spectral hole burning and spectral holography. Up to 100,000 bits per spot are expected during our development cycle. Very preliminary university demonstrations have already achieved more that 4000 bits per spatial location. Because of the high multiplicity of bits within a single spatial address, substantial data capacities can be achieved with a relatively small number of spatial addresses.

Multi Gigabyte (50-100) capacity storage units can be implemented with entirely non-mechanical beam steering, thus providing random access times of microseconds rather than the random access times of milliseconds common in mechanically accessed magnetic disk storage technology.

ODRAM is based on two technologies, spectral holography and persistent spectral hole burning. Spectral holography refers to the recording of temporal waveform information in the frequency dimension within frequency selective recording materials. Spectral holography is effected through the spectral interference of distinct temporally structured (data encoded) light beams inside the recording material. Persistent spectral hole burning refers to the physical process of modifying the absorption profile of frequency selective materials, recording the information.

Technical Objectives of Phase I and Interim Funding Periods

Design, implement, and evaluate components and subsystems for development of an optical dynamic RAM and begin development of a laboratory demonstration unit. (No change to previously stated objectives).

The overall, long-term goal of Templex Technology is the integration of the recently **demonstrated** high multiplicity spectral multiplexing with **existing** non-mechanical beam-deflection technology to yield a high capacity, low latency, Optical Dynamic RAM. The possibility of ODRAM class memory was first suggested after the demonstrations of multi-kilobit spectral multiplexing of data at single spatial locations. Without dense spectral (or some other type of) multiplexing, it is impossible to non-mechanically access useful amounts of data with current optical beam control technologies. The ODRAM concept integrates a variety of optical and other technologies in new combinations, subject to new constraints. Templex Technology's overall Phase I objectives were to:

- Determine the ODRAM performance levels that can be realized on a short-term basis by designing and performing an exhaustive performance analysis of an ODRAM prototype, as achievable using existing storage materials and optical support technology. These results would form the basis of Phase II SBIR work where prototypes will actually be constructed and tested.

- Determine prototype and production level costs associated with currently realizable Optical RAM devices.

- Conduct laboratory evaluation of potential high performance storage materials.

- Evaluate the probable future course of storage material development and determine Optical RAM performance when implemented with materials projected to be available.

Templex Technology's Interim objectives were to:

- Develop a laser for use in ODRAM with improved performance relative to the laser used during Phase I.

- Construct interface and control unit for ODRAM with improved performance relative to the interface and control unit used during Phase I.

- Integrate improved laser and interface and control unit into ODRAM demonstration unit.

Work Performed and Results Obtained

Our analyses of potential performance and cost structure during Phase I have been very positive. Based on these analyses, we believe that we can build a device that has an enormous performance advantage relative to magnetic storage media with a cost per GByte that is significantly below the cost per GByte of semiconductor DRAM. We were very encouraged by these results and have rapidly moved beyond the paper-based analyses to design and construction of an initial laboratory-demonstration unit, which we had originally planned to begin during Phase II. Our key findings and results are detailed below.

1) *Potential ODRAM Device Performance.* The major advantage of ODRAM relative to existing and entrenched memory technologies is a combination of speed and capacity for a competitive price. We have estimated that the unit cost in early production will be in the range of $20,000-25,000 for 100 Gigabytes of capacity. The nonmechanical access of ODRAM will enable much higher data throughput rates and much faster access to small records in large databases. ODRAM offers up to three orders of magnitude of improvement in data access rates relative to mechanically-accessed memory technologies. The combination of nonmechanical data access and parallel data access opens the possibility of average transfer rates exceeding silicon DRAM.

Large Capacity: ODRAM achieves high storage capacity, as well as high storage density, by storing large numbers of bits in every spatial location, using a unique combination of time and frequency domain multiplexing (swept-carrier memory, see below). In brief, temporal data sequences are stored in a storage material capable of discriminating different colors of light, *i.e.*, a spectrally selective material. At the heart of ODRAM is a small crystal (on the order of 75×75×1 mm^3) of a spectrally selective material, used as the recording material. This crystal is divided into separate spatial storage locations accessed by acousto-optic beam deflection. In one of the planned prototypes, whose parameters will be treated as an example, there will be 9,000,000 spatial storage locations arranged in a 3000 × 3000 grid filling the face of the crystal. Each individual storage location will hold 100,000 temporally multiplexed bits, yielding a capacity of more than 100 Gigabytes. In terms of storage density, this corresponds to a volume density of 160 Gigabits/cm^3 or, since the spatial cells are distributed in a two dimensional grid, an areal density of 100 Gigabits/in^2. Note that these

densities are very low compared to the maximum densities achievable with the ODRAM technology, indicating that future implementations may utilize storage densities one or more orders of magnitude greater than our current targets. We note further, however, that the densities mentioned are of secondary importance compared to the overall storage capacity since it is the latter quantity that largely determines the overall cost/unit performance.

Fast Random Access Rates: ODRAM utilizes an entirely nonmechanical approach to data access. As a result, ODRAM provides random access speeds nearly 1000-fold faster than mechanically addressed data storage devices. In particular, the 9,000,000 spatial storage locations will be accessed via acousto-optic beam deflection, with a projected latency time of 20 microseconds (to be compared to the 5-10 millisecond latency of a magnetic hard drive). This 20 microsecond latency is determined by the acoustic velocity in the acousto-optic beam deflector and is consistent with current commercially available technology. In addition to shortening the latency associated with random access, the ODRAM architecture eliminates latencies inherent in interconversion between storage and electronic bus formats. This is achieved by operating in a high-speed 64-bit parallel mode (post Phase II development extending the proposed 8-bit bus) that exploits the parallelism of optics while allowing direct interfacing with existing computer architectures. Note that future ODRAM units will be designed with more parallel channels to match wider data busses in future computers.

High Speed Average Transfer Rates: The overall data transfer rate of a memory technology is determined by both its random access latency time and its peak data transfer rate. ODRAM will offer high peak data transfer rates in addition to the short latency times discussed above. ODRAM will achieve high peak data transfer rates (on the order of 2 Gigabits/second) by parallel operation of 64 channels, each running at an electronically convenient 30 megabits/second. It is anticipated that ODRAM will eventually be implemented (post Phase II) with single channel bit

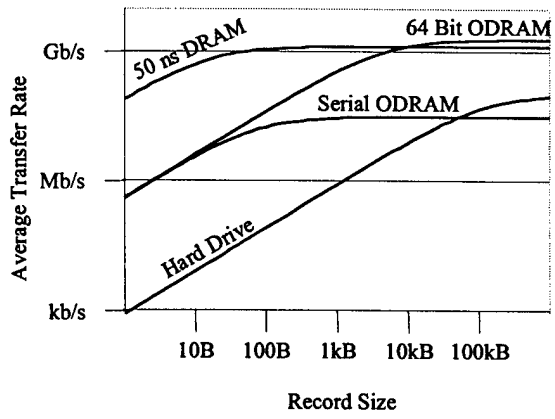

Figure 1. Average transfer rate as a function of record size. The average transfer rate for a given technology represents the total data throughput rate for that technology, taking into account the latency, the single channel bandwidth, and the number of parallel channels utilized. Here, ODRAM is assumed to have a single channel bandwidth of 30 megabits/second with a latency of 20 microseconds.

rates as high as 1 Gigabit/second, and bus aggregate peak data rates of 64 Gigabits/second. In Figure 1, we plot the average transfer rate (which is affected by both latency and peak transfer rate) as a function of record size for several technologies. For contiguous records smaller than 50 kilobytes, ***Serial*** ODRAM running at 30 megabits/second with a 20 microsecond latency offers higher average transfer rates than can be achieved with a magnetic hard drive. ***64-bit-parallel*** ODRAM offers data transfer rates orders of magnitude larger than those achievable with hard drives for any record length. Interestingly enough, even though the latency time of ODRAM is longer than silicon DRAM, the average throughput of ODRAM exceeds the average throughput of 50 nanosecond 64-bit-wide DRAM for contiguous records greater than 10 kilobytes.

High-Speed Writing: Templex Technology's implementation of ODRAM will utilize materials that are compatible with high-speed writing. The data rates listed in the previous section apply to **both** the read and write functions. High-speed writing is possible through the use of rare-earth doped crystalline materials as the spectrally selective recording material. These materials display quantum efficiencies for writing in the range of 50%, enabling high-speed writing.

2) *Materials Characterization of Eu^{3+}:Y_2SiO_5.* Our preliminary literature studies (a partial summary is given in Table 1), along with extensive discussions with Rufus Cone (University of Montana), Randy Equall (Scientific Materials), and Ralph Hutcheson (Scientific Materials), led us to believe that Eu^{3+}:Y_2SiO_5 would be an almost ideal material for development of ODRAM, due to the long data storage time and the high potential capacity. The one disadvantage is the transition wavelength, which is not directly accessible with a commercially available diode laser.

Completion of test bed for studying Eu^{3+}:Y_2SiO_5. Material properties of Eu^{3+}:Y_2SiO_5 were studied using a combination of two and three pulse photon echoes as a function of temperature, excitation intensity, and incident polarization. Eu^{3+} substitutes into two different sites of Y_2SiO_5, leading to transitions at 580.036 nm (Site 1) and 580.209 nm (Site 2). Both sites were studied in two separate samples, a 2 mm thick sample with a 0.5% doping level and a 1 mm thick sample with a 1% doping level. The optical pulses were generated by acoustooptic chopping of the $\approx$ 580 nm output of a commercial (Coherent 699) dye laser. The Eu^{3+}:Y_2SiO_5 samples were cooled to subambient temperatures by contact with a cold finger that was cooled by contact with flowing liquid helium. Temperature control was maintained by resistive heating of the cold finger above the boiling point of helium. Photon echoes were detected using a Hamamatsu avalanche photodiode, model # C5331.

Table 1. Figures of merit for representative frequency selective materials

Material	*Temperature*	Γ_H	Γ_I	*Storage Time*	*Mechanism*	*Refs*
$Eu^{3+}:Y_2SiO_5$	1.4 K	100-200 Hz	4 GHz	Hours to days	Hyperfine	1
	6 K	300-400 Hz	6-9 GHz	Hours to days		2-4
$Eu^{3+}:Y_2O_3$	4 K	3 kHz		>30 hours	Hyperfine	5
	14 K	300 kHz		5 seconds		5
	1.4 K	0.8-42 KHz				6
$Tm^{3+}:LaF_3$	1.5 K	45 kHz	4 GHz	10 ms	Metastable	7-8
Tm^{3+}:YAG	1.5 K	4 kHz		10 ms	Metastable	8
$Pr^{3+}:Y_2SiO_5$	1.4 K	1-2 kHz	3-4 GHz		Hyperfine	9
Eu^{3+}:Silicate glass	0.4-4.2 K	2 MHz-10 MHz		> 100 s at 1.2 K	Hyperfine	10
Pr^{3+}:Silicate glass	0.4-10 K	10 MHz-700 MHz		> 100 s at 1.2 K	Hyperfine and persistence	10
Eu^{3+}: β''alumina	5 K	1 GHz		2 minutes	Hyperfine	11
	110 K	10 GHz		30 minutes	Ionic motion	
Sm^{2+}:BaFCl	2 K	25 MHz	16 GHz	"permanent"	Photon gated	12
$Sm^{2+}:BaFCl_{.5}Br_{.5}$	77 K	1.4 cm^{-1}	26 cm^{-1}	"permanent"	Photon gated	13
$Sm^{2+}:SrFCl_xBr_{1-x}$	295 K	200 GHz		"permanent"	Photon gated	14
Sm^{2+}:SrFCl	77 K	0.4 cm^{-1}		"permanent"	Photon gated	15
$Sm^{2+}:SrFCl_{.5}Br_{.5}$	295 K	4 cm^{-1}	30 cm^{-1}	"permanent"	Photon gated	16
$Pr^{3+}:D^-:SrF_2$	1.6 K	<1 MHz		minutes	D^- migration	17

Table 1 References

1) R.W. Equall, Y. Sun, R.L. Cone, R.M. Macfarlane, Phys. Rev. Lett., **72**, 2179 (1994)
2) R. Yano, M. Mitsunaga, N. Uesugi, J. Opt. Soc. Am., **9**, 992 (1992)
3) R. Yano, M. Mitsunaga, N. Uesugi, Opt. Lett., **16**, 1884 (1991)
4) R. Yano, M. Mitsunaga, N. Uesugi, Opt. Lett., **16**, 1890 (1991)
5) W. R. Babbitt, A. Lezama, T.W. Mossberg, Phys. Rev. B, **39**, 1987 (1989)
6) G.P. Flinn, K.W. Jang, J. Ganem, M.L. Jones, R.S. Meltzer, R.M. Macfarlane, J. Lumin., **58**,374 (1994)
7) R.M. Macfarlane, Opt. Lett., **18**, 829 (1993)
8) R.M. Macfarlane, Opt. Lett., **18**, 1958 (1993)
9) R.W. Equall, R.L. Cone, R.M. Macfarlane, Phys. Rev. B, **52**, 3963 (1995)
10) Th. Schmidt, R.M. Macfarlane, S. Volker, Phys. Rev. B, **50**, 15707 (1994)
11) H. Yagumi, R. Yagi, S. Matsuo, M. Ishigame, Phys. Rev. B., **53**, 8283 (1996)
12) A. Winnacker, R.M. Shelby, R.M. Macfarlane, Opt. Lett., **10**, 350 (1985)
13) C. Wei, S. Huang, J. Yu, J. Lumin., **43**, 161 (1989)
14) T. Asatsuma, N. Umezu, Y. Takemoto, M. Kaneko, J. Lumin., **64**, 201 (1995)
15) J. Zhang, S. Huang, W. Qin, D. Gao, J. Yu, J. Lumin., **53**, 275 (1992)
16) N. Umezu, T. Asatsuma, Y. Takemoto, M. Kaneko, **64**, 195 (1995)
17) R.J. Reeves, R.M. Macfarlane, Phys. Rev. B, **47**, 158 (1993)

Photon echoes. Two pulse photon echoes were used to characterize the homogeneous and inhomogeneous linewidths, which can be used in the calculation of potential device capacity. As an example, a plot of the homogeneous linewidth, measured as a function of excitation intensity at several different temperatures is shown in Figure 2. Figure 3, which is slightly simpler, shows the measured homogeneous linewidth as a function of temperature for a single excitation intensity, 1100 W/cm^2. As expected, the linewidth increases with increasing temperature and with increasing excitation intensity. More

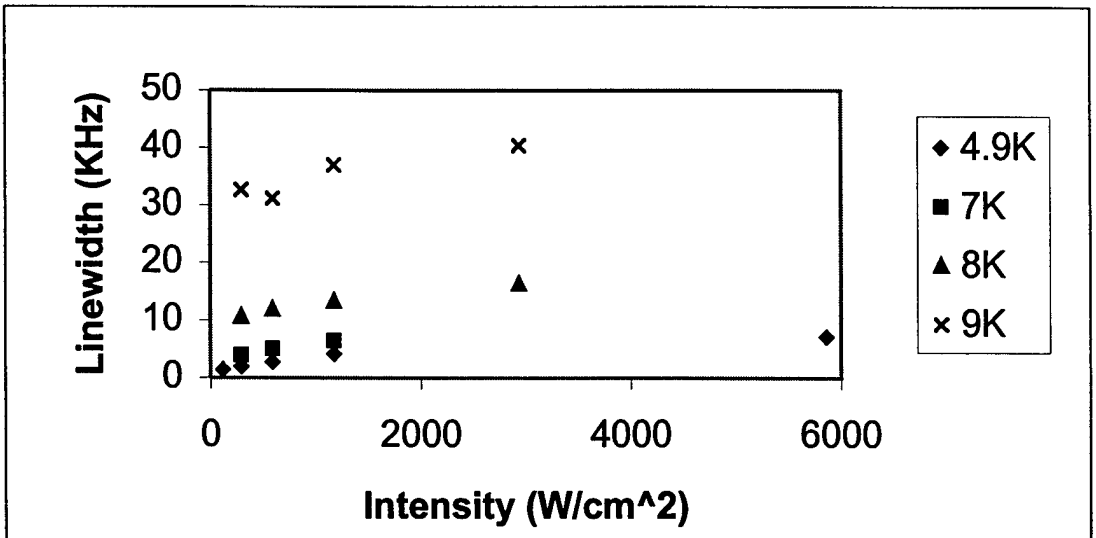

Figure 2. Homogeneous linewidth of $Eu^{3+}:Y_2SiO_5$ as a excitation intensity at several representative temperatures. Results shown here are for Site 1 of the 2 mm, 0.5% doped sample.

importantly, the results of two pulse photon echo studies indicate that the effect of excitation intensity on the homogeneous linewidth (instantaneous diffusion or excitation induced dephasing) is not a function of temperature. At low temperatures, excitation induced dephasing can contribute to a large fractional change in homogeneous linewidth. However, excitation induced dephasing only causes a small fractional change at higher temperatures (~10K). The dependence of the observed linewidth on excitation intensity is linear at low intensity and shows saturation behavior at higher intensities.

Three pulse photon echoes were performed in site 1 of the 1 mm thick 1% sample at temperatures up to 9 K. In this case, the delay times (between the second and third pulses) were varied from 25 μs to 9.5 ms. The echo intensity decreased from 306 mV at short delays to 45 mV at long delays. Note that 9.5 ms is much longer than the excited state lifetime of 1.9 ms for site 1. The ratio of the intensity at short time to the intensity at long time (relative to the excited state lifetime) indicates a quantum yield for persistent hole burning

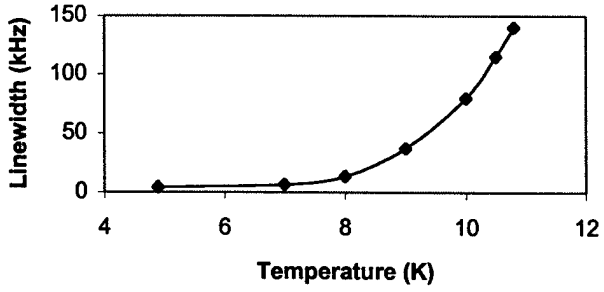

Figure 3. Linewidth as a function of temperature. Results shown here are for an excitation intensity of 1100 W/cm^2 of Site 1 of the 2 mm, 0.5% doped sample.

of approximately 50%. This is a very important and very encouraging result, as this high quantum yield will enable rapid writing in a practical memory device. If the quantum yield were significantly lower, as is common for many organic and inorganic molecular systems, rapid writing would not be readily achievable.

Larger signals were observed in the 2 mm thick 0.5% sample. This difference is due to a combination of a different optical polarization relative to the crystalline axes and an intrinsically higher peak optical density in the lower concentration sample. Polarization dependent studies in the 2 mm thick 0.5% sample indicate a pronounced polarization dependence, approaching an optical density of 0 at some angles in site 1.

3) *Construction of a laboratory demonstration unit* for swept carrier data storage and recall in $Eu^{3+}:Y_2SiO_5$. As mentioned above, our initial Phase I results were extremely encouraging, leading us to begin laboratory prototype development during Phase I, rather than waiting for the commencement of Phase II.

The general architecture of ODRAM is summarized in Figure 4. In brief, digital data is encoded onto a frequency agile optical carrier by the data encoder and directed to a particular spatial address within the storage material by the X-Y A/O deflector. In each and every spatial location of the storage material, tens to hundreds of thousands of bits are stored with spectral holographic techniques. Readout is achieved by illumination of the appropriate spatial location with a reference wave that generates a replica of the stored optical bit-sequence. This output optical bit sequence is detected and electronically processed to yield a digital electronic data sequence.

Frequency Agile Laser: During the Phase I and Interim periods, we have constructed and utilized two different frequency agile lasers and started

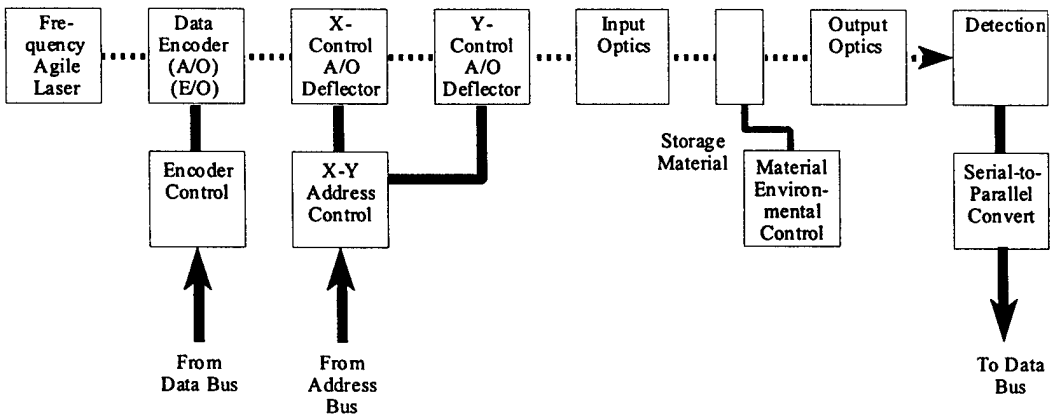

Figure 4. Block diagram of the major optical components and subsystems for ODRAM.

construction of a third. Frequency sweeping is obtained through the use of an acousto-optic modulator in one embodiment and through the use of intracavity tuning elements in the other two embodiments. Note that a dye laser is a short term solution to the requirement of a frequency agile laser. Commercial ODRAM products will incorporate a frequency agile laser that is based on solid state and/or semiconductor components for ruggedness.

The first generation laser utilized an acousto-optic modulator to frequency chirp the output of a commercial ring dye laser. In particular, sweeping was accomplished by double passing the output of the dye laser through an acousto-optic modulator with an applied RF field that is frequency chirped. Over 100 MHz of tuning is obtained in this fashion. While 100 MHz was sufficient for the initial demonstrations discussed below, a tuning range of several GHz is required to fully utilize the inhomogeneous bandwidth of the storage material. In addition, this method introduces a small spatial beam walk, which limits the output signal size, and thereby the output signal to noise ratio.

The second generation laser utilized intracavity electro-optic crystals to generate a frequency chirp. With this laser, we achieved an extended tuning range (relative to the acousto-optic tuning method) without complications of time- and frequency-dependent spatial beam walkoff.

Our initial design for the second-generation laser utilized a two-mirror cavity with a birefringent filter, an etalon, and an electro-optic crystal for rapid tuning. This design was difficult due to large coupling between multiple degrees of freedom in the cavity, which did not allow for individual optimization of any given component. In addition, the wavelength selective elements did not perform well, because they were not placed in a collimated beam, due to the lack of a collimated section in the two-mirror cavity. Frequency agile performance was not achieved with this cavity design.

Our subsequent design for the second generation laser utilizes a three-mirror cavity and allows for individual optimization of every component. In addition, the wavelength selective elements are placed in a collimated region of the cavity, allowing for optimal performance. Using a birefringent filter and two etalons for wavelength selection, we observed mode-hop free tuning that appeared to be limited by the etalon loss curves to less than one free spectral range of 450 MHz. Frequency agility greater than one free spectral range was obtained by simultaneous scanning of a two intracavity electro-optic crystals. The first electro-optic crystal simply modified the effective cavity length, while the second electro-optic crystal, which had partial reflection coatings on both ends, acted as a rapidly tunable etalon. The tuning range was limited by the available voltage source and by the half-wave voltage of the electro-optic tuning crystal.

The third generation laser, which became operational at the end of the period covered by this report, combines the optics of a commercial ring dye laser with custom electronics to simultaneously achieve frequency agility and long-term

frequency stability. In brief, the dye laser is stabilized to an external cavity using the Pound-Drever-Hall approach (R.W.P. Drever, J.L. Hall, F.V. Kowalski, J. Hough, G.M. Ford, A.J. Munley, H. Ward, Appl. Phys. B, **31**, 97 (1983).) Frequency agility is obtained by scanning the reference cavity and forcing the dye laser to follow. The elements that are being used to scan the dye laser include a Brewster plate mounted on a galvanometer, a mirror mounted on a piezoelectric transducer, and an etalon. Feedback signals derived from the error signal are applied to the galvanometer and the piezoelectric transducer. Additional "feedforward" signals are also applied to these elements, to enable a fuller utilization of the dynamic range of the error signal. A "feedforward" signal is also applied to the thick etalon. With this laser, we have observed frequency stabilized sweeps of 5 GHz and peak slew rates greater than 2 MHz/μs. For comparison, the maximum slew rate obtainable using the commercial electronics is about 100 kHz/μs.

Data Encoder: Data and reference beams are generated using acousto-optic modulators. In one embodiment, the acousto-optic modulator is driven with two RF fields, a CW field generating the reference and a modulated field generating the data. For low frequency offsets, the two output beams are collinear within the diffraction limit. To generate collinear beams with large frequency offsets, the data and reference beams are generated in separate acousto-optic modulators and are subsequently combined on a beam splitter.

Detection: As the data and reference beams are collinear, the generated output beam is collinear with the read beam. The heterodyne beat signal between the output and read beams is detected on a photodiode, generating an electronic replica of the optical heterodyne signal. This electronic heterodyne signal is processed using envelope detection to generate a bit stream which is subsequently downloaded to the control computer.

Data Storage Results: The initial attempt resulted in storage and recall of 14 bits. In this case, the signal detection limit was better than 10^{-5} (ratio of reconstructed signal intensity to data intensity). In subsequent efforts we stored and recalled 200 bits, achieving a spectral density of 2 bits/MHz, matching previous University of Oregon demonstrations using Tm^{3+}:YAG. Representative data for low and high spectral density are shown in Figure 6 and Figure 5, respectively. The bit count

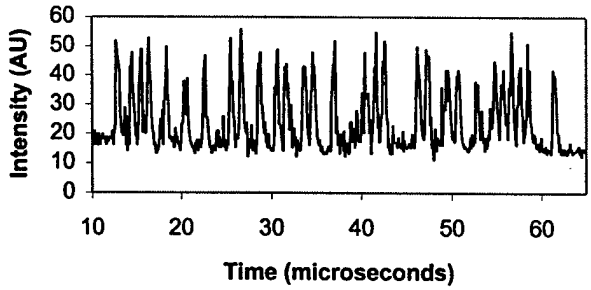

Figure 5. Representative bits stored and recalled using heterodyne detection under conditions of high spectral density.

of 200 bits/spot was limited by the smallness of the laser tuning range implemented in that particular demonstration (using the acousto-optically swept frequency agile laser). It should be noted, however, that we have broken the previous record for the number of bits recalled and for the achieved spectral density using heterodyne techniques. In this particular measurement, the measured signal to noise ratio of the electronic signal following envelope detection was greater than 4. It is important to note, however, that the output signal intensities were over one order of magnitude lower than expected. This decrease in signal intensity was determined to be due to the acoustooptic frequency sweeping method. In particular, there is a decrease in the spectral/spatial overlap of the data and reference beams due to a slight beam-walk induced by the acousto-optic modulator.

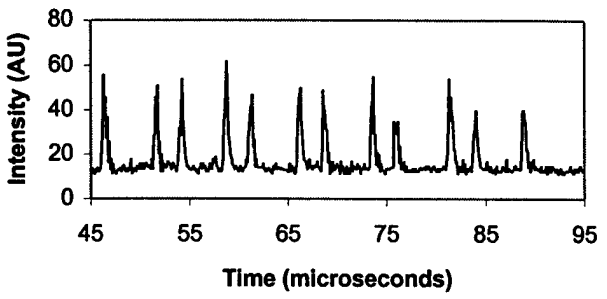

Figure 6. Representative bits stored and recalled using heterodyne detection under conditions of low spectral density.

Upon replacement of the acousto-optically swept frequency agile laser with the second generation, electro-optically swept frequency agile laser, we could observed output signal efficiencies of the expected magnitude. This is consistent with our theory that beam walk induced by the acousto-optic modulator was responsible for the reduced output efficiency observed previously. Note that the output signal efficiency was high only under certain conditions. In particular, the output signal intensity was strongly attenuated if the storage material was irradiated as the laser frequency was swept back to the starting frequency between the data storage cycle and the data readout cycle. This has been interpreted as an indication of data erasure during the frequency "rewind" cycle. We did not achieve high bit/spot counts with this second generation laser due to long term (100 microsecond and longer) frequency drift.

4) *Maintained external contacts with Scientific Materials and Montana State University.* The collaborative studies between Scientific Materials and Montana State University have long been important in the development and characterization of new memory materials. For example, measurements by Y. Sun in the laboratory of Rufus Cone indicate that the inhomogeneous linewidth of Eu^{3+}:Y_2SiO_5 is a very strong function of concentration and that the absorption cross sections are strongly polarization dependent. Our results are in qualitative agreement. (A quantitative comparison has not yet been made.)

Personnel Supported:

Alan E. Johnson
Eric Maniloff
Thomas W. Mossberg

Publications:

No peer reviewed publications have been submitted during the time period covered by this report.

Interactions/Transitions:

1. Attended 1997 CEC/ICMC 1997 (Cryogenic Engineering Conference & International Cryogenic Materials Conference) and presented a paper entitled "Cryogenically Cooled Optical Dynamic RAM".
2. Attended 1997 Optical Society of America Annual Meeting and presented a paper entitled "Optical Dynamic RAM: A New Entry in the Memory Hierarchy".
3. Attended 1998 Workshop on Applications Spectral Hole Burning and presented a paper entitled "The Templex Technology Optical Dynamic RAM Project".
4. Attended 1998 SPIE meeting and presented a paper entitled "A high-speed implementation of spectral memories: Optical Dynamic RAM.".
5. Attended Workshop on High Density Optical Data Storage and presented a paper entitled "Spectral Hole Burning Data Storage".
6. Attended Workshop on Optical Devices Using Rare Earths and Other Novel Approaches and presented a paper entitled "Spectral Hole Burning Data Storage in Rare Earth Doped Crystals".

New discoveries, inventions, or patent disclosures:

Novel method of attaining frequency agile performance from a dye laser or other laser with a very broad gain profile utilizing electro-optic etalons.
Novel method of laser stabilization using a fiber interferometer (in conjunction with University of Oregon researchers under Prof. T.W. Mossberg)

Honors/Awards:

None during the period covered by this report.

Future Directions

Initial efforts during Phase II will involve integration of the third generation frequency agile laser to achieve a high per-spot storage density. In general, during Phase II we will continue development of ODRAM, pushing the limits of the technology to achieve higher single spot bit counts, nonmechanical spatial addressing, dynamic refresh, and parallel data access. Full details of the Phase II work plan were presented in the Phase II proposal.